Technical University of Denmark

DTU

Sensitivity of Nodal Admittances in an Offshore Wind Power Plant to Parametric Variations in the Collection Grid

Vytautas, Kersiulis; Holdyk, Andrzej; Holbøll, Joachim; Arana, Ivan

Link back to DTU Orbit

DTU Library
Technical Information Center of Denmark

Sensitivity of Nodal Admittances in an Offshore Wind Power Plant to Parametric Variations in the Collection Grid

Vytautas Kersiulis
Technical University of Denmark
vytautas.kersiulis@gmail.com

Andrzej Holdyk
Technical University of Denmark
aho@elektro.dtu.dk

Joachim Holboell
Technical University of Denmark
jh@elektro.dtu.dk

Ivan Arana
DONG Energy
ivaar@dongenergy.dk

Abstract-- **The paper presents sensitivity studies on nodal admittances in the offshore wind farm to different parameters of the collection grid cable system, including length of cable sections and actual layout configuration. The main aspect of this investigation is to see how parametric variations influence admittance and, consequently, voltage transfer in frequency domain. The simulation model of the offshore wind farm was build based on the main components in turbines and the collection grid. The simulation results were compared with data from time domain measurements and showed good agreement. A number of nodes were selected for evaluation of the admittances: the connection point to the external grid, a point at the substation and at each wind turbine. The results show that at specific locations resonances occur, where the admittance increases significantly in the 10-100 kHz range, depending on the location. On the other hand, anti-resonance peaks occur in the 0.1-10 kHz range and these are not location dependent. Resonant peaks at higher frequencies are proved to be determined mainly by collection grid cables. Voltage transfer measurements from the wind turbines low voltage side to the external grid connection show that high frequency components are highly damped at that distance. A considerable match was found between high frequency peaks in the admittance scans and the voltage transfer at the collection grid. This proves that some particular frequencies cause series resonances to occur at particular locations at the wind turbines medium voltage side**.

Index Terms—**Offshore wind farms, nodal admittance, cable, resonances.**

I. INTRODUCTION

The connection topology of electric components in an offshore wind farm (OWF) is unusual and very compact when compared to regular electric networks. One of the main challenges when building an offshore wind power plant is defining the design and building the internal sub-sea cable grid interconnecting the wind turbines - the collection grid [1]. Due to their design these cables have a capacitive component which can interact with other components, e.g. transformers, filters, loads, and cause resonances [2]. Also resonances with the cables own inductance occur. To investigate the sensitivity of electrical conditions in offshore wind farms to changes in some parameters of the collection grid cables, a frequency dependent model is necessary. For this purpose an offshore wind farm has been modelled based on main components in turbines and collection grid including frequency-dependent cable and transformer models.

Driving-point admittance and voltage transfer methods are used in order to investigate possible resonances occurring at different locations in the farm. Particular models for simulation studies are chosen, since the investigation of frequency sweeps and voltage transfer is done in a broad frequency range. The study identifies possible resonances occurring at the system as well as critical resonant locations by comparing admittance scans and transferred voltages. The understanding of behaviour and dependency of resonances on the topology of the collection grid can be useful in the future projects, in order to reduce risk of generation of critical overvoltages and increase reliability of the electrical system.

ATP-EMTP software is used for modelling electrical components.

II. WIND FARM DESCRIPTION

The electrical system of the investigated offshore wind farm consists of five main elements:
- Point of Common Coupling
- Onshore substation together with onshore transmission cables
- Transmission cables to shore
- Offshore inter-turbine cables (collection grid cables)
- Wind turbine generators with wind turbine transformers

The OWF consists of 25 wind turbines, connected in three radials to an onshore substation. The onshore substation contains the main park transformer (90 MVA, 132/33 kV) which connects the wind farm with external grid by means of high voltage transmission cables and overhead lines. This substation also contains a reactive power compensator – a capacitor bank (12 MVAr, 33 kV) and an auxiliary transformer (150 kVA, 33/0.415 kV) with an auxiliary load of 80 kW at 0.415 kV. Four different cable types were used in the collection grid: 800 mm^2, 500 mm^2, 240 mm^2, 95 mm^2. Estimated distance between turbines is 700 m and 900 m between the radials. Each wind turbine contains a wind turbine transformer (4 MVA, 34/0.69 kV), together with an auxiliary load, a high frequency filter and an inverter reactor - all components connected at the low voltage side together with induction generator. In addition to that, each wind turbine is supplied with a circuit breaker at both medium voltage (MV) and low voltage (LV) side of the wind turbine

transformer. Each of the 3 radials is connected to the substation through a circuit breaker.

A single line diagram of the whole wind farm is shown in Fig. 1. The upper part is the substation with the 2 busbars plus transformers and the capacitor bank. Each turbine at a radial is identified with an individual number from "Wind turbine 1" (WT1) to "Wind turbine *n*". The measurement locations are indicated as red dots in Fig. 1.
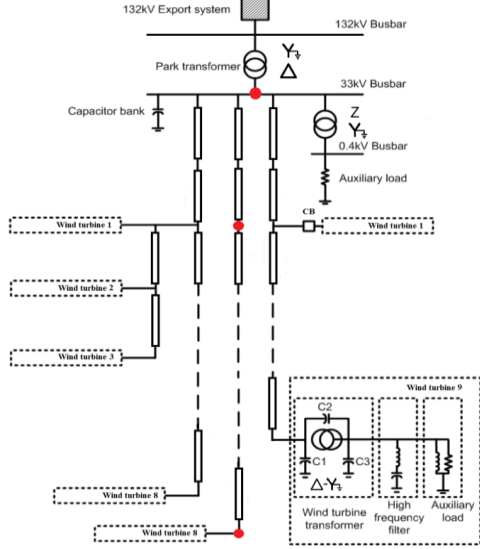

Fig. 1 Single line diagram of the offshore wind farm model. Measurement locations indicated as red dots.

III. THE MODEL

To investigate the electrical conditions at the specified locations in the farm, a model was build using standard electrical component models. The ATP-EMTP software provides frequency dependent cable models and transformer models with topologically-correct core implementation, where an optional frequency dependent winding resistance is available.

The wind farm model is described in more details in [3].

This model is validated by comparing time domain signals from simulation data with measurement data from the OWF. These data were obtained during energisation of the middle radial. Simulation and measurement results at the substation are compared in Fig. 2.
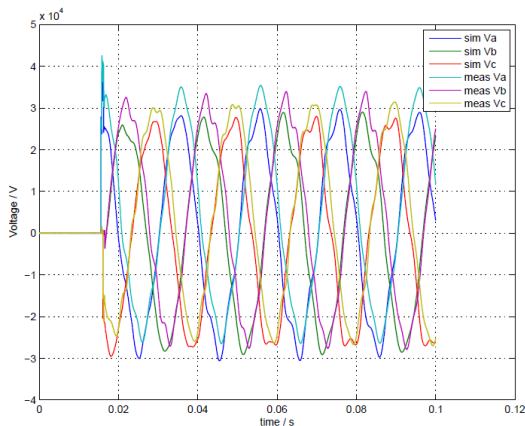

Fig. 2 Measured (*meas*) and simulated (*sim*) voltages at the substation during middle radial energisation.

Fig. 3 shows voltage at the substation during middle radial energisation, where measured and simulation data are compared.
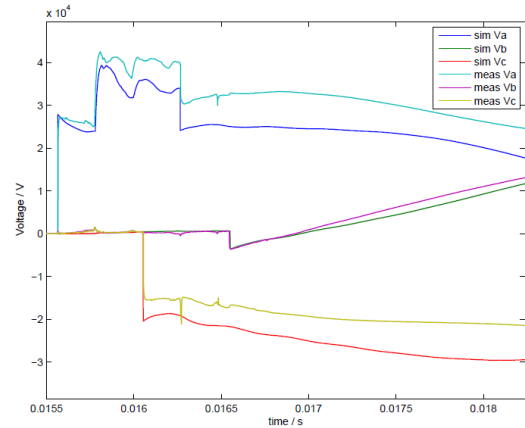

Fig. 3 Measured (*meas*) and simulated (*sim*) voltages at the substation during middle radial energisation with focus on the switching process.

Fig. 2 and Fig. 3 show almost similar voltages at the substation when measurement and simulation results are compared. Some transformer saturation effects are visible, as well as accurate damping of the switching overvoltages at phase A, caused by a prestrike. The differences in measured and simulated voltages are most likely due to transformers saturation characteristic and it does not influence the main results of this study, where the performed frequency sweeps are done for a linear model. Also, there is no influence of phenomena related to circuit breaker operation on the frequency sweeps; therefore, the vacuum circuit breaker was modelled as an ideal switch. The prestrike phenomenon was also modelled in time domain, but only for validation purposes, by manually opening and closing of the switch. More detailed validation of the model is shown in [4].

IV. SIMULATION METHODS

The main investigation points were chosen to be at medium voltage and low voltage side at each wind turbine at the middle radial. This was done in order to be able to compare possible resonances at the wind turbines and at the collection grid, as well as to indicate locations with possible worst overvoltage conditions. In many studies [1] it is assumed that the worst overvoltages occur at the last or first wind turbine in a radial. In order to give a thorough picture, in this study each wind turbine location at a selected radial was investigated.

Looking at admittance and impedance scans, series and parallel resonances give different characteristics. Parallel resonance is caused by parallel connection of inductive and capacitive elements and causes the characteristic impedance to be very high, as long as the resistive part is ignored. Under such conditions, high overvoltages can occur, even with very small currents injected. Such a situation is also called anti-resonance condition. Series resonances occur when the same components are connected in series. At resonance frequency, the reactance of inductor almost cancels out the reactance of

capacitor and high currents can occur even with very small voltages applied.

In the study, the parameters to be varied were: lengths of cable sections and actual configuration of the offshore wind farm, e.g. changing cable types for interconnecting wind turbines and disconnecting main components at the substation. This allows identifying which components or parameters are influencing resonances the most.

The frequency response of a particular node's driving-point admittance is calculated by connecting a sinusoidal voltage source to the node with amplitude of one volt and measuring the current flowing into the network for different frequencies. Measurement of voltage transfer is done by connecting a sinusoidal voltage source at one node and measuring the voltage transferred to another node. Both properties can be calculated in frequency domain.

V. RESULTS

Multiple locations were chosen for investigation of the driving-point admittance, see Fig. 4, where the main observations are presented.
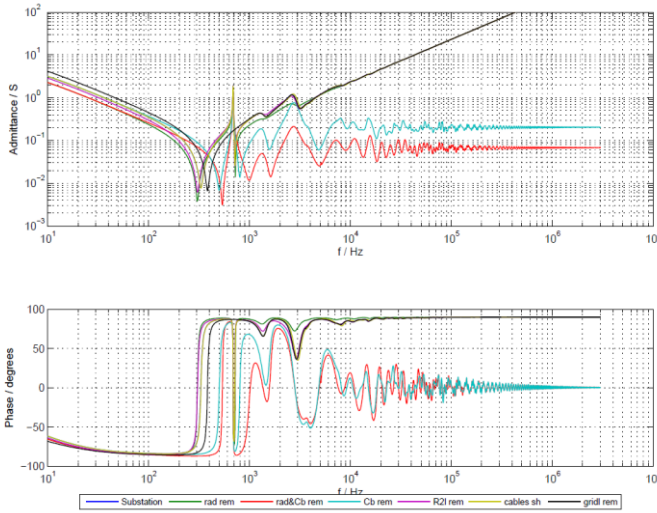
A. Admittance scans

Fig. 4: Driving-point admittance at the onshore substation.

rad rem - side radials are disconnected and only middle radial is left; *radCb&rem* - side radials are disconnected together with capacitor bank; *Cb rem* - side radials are connected and capacitor bank is disconnected; *R2l rem* - high frequency filters with reactors and auxiliary loads are disconnected at each wind turbine at the middle radial; *cables sh* - all cables connecting wind turbines at middle radial are shortened from 700 m and 900 m to 600 m and 800 m, respectively; *gridl rem* - external grid impedance is removed.

It is seen how different components affect the admittance in different frequency ranges. Removal of side radials → admittance decrease up to 3 kHz range and 330 Hz peak shift to lower frequencies; removal of a capacitor bank → resonant peaks shift to higher frequencies as an indication of resonances at higher frequencies caused by the collection grid cables; removal of loads at low voltage side of wind turbines

at middle radial → admittance value decrease and 330 Hz peak shift to lower frequencies; shortening of collection grid cables → small influence on admittance shift in frequency; removal of grid impedance → disabling 715 Hz peak.

Fig. 5 shows the admittance scan at the MV side of each wind turbine at the middle radial. For comparison the same admittance scan is plotted when the cable length connecting WT7 and WT6 is shortened by 100 m.
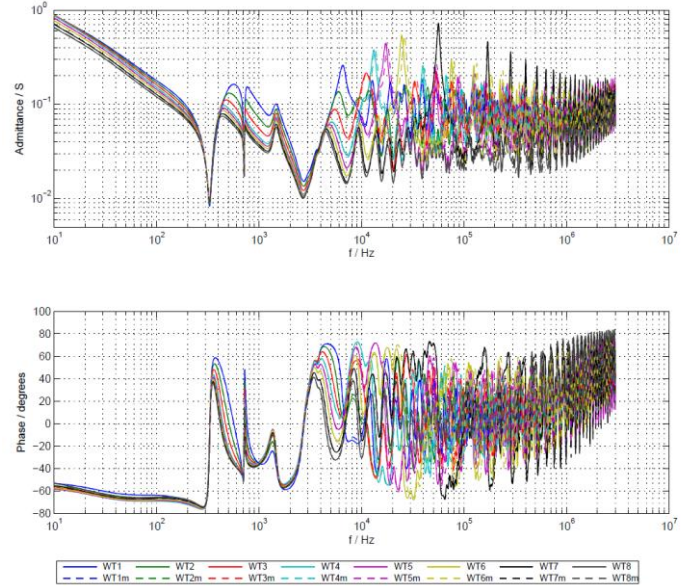

Fig. 5: Admittance scan at the middle radial at each wind turbine compared with the same scan when cable length connecting WT7 and WT6 is shortened by 100 m. *WTn* – measurement location; *WTnm* – modified measurement, where n is the wind turbine number.

Here anti-resonant frequencies are identified at 330 Hz, 715 Hz and 2.75 kHz. Sharp resonant peaks appear at higher frequencies: 56.23 kHz at WT7, 24.66 kHz at WT6, 16.98 kHz at WT5 and 13.12 kHz at WT4. The shorter cable between WT7 and WT6 causes clear frequency shifts at WT4, WT5 and WT6 - Δf_{WT4} = 492 Hz, Δf_{WT5} = 807 Hz, Δf_{WT6} = 1642 Hz.

Fig. 6 shows admittance scan performed at the WT7 location, where a sharp resonance was observed at 56.23 kHz. Here similar configurations as at substation location are used. The figure indicates that the resonant peaks at higher frequencies are not influenced by the main onshore substation components, where only the anti-resonant peaks at 330 Hz, 715 Hz and 2.75 kHz are affected. A small effect on admittance is visible when the middle radial loads at the low voltage side are removed. This causes a shift of the admittance to higher frequencies, the 56.23 kHz peak shift is now Δf_{WT7} = 2110 Hz.
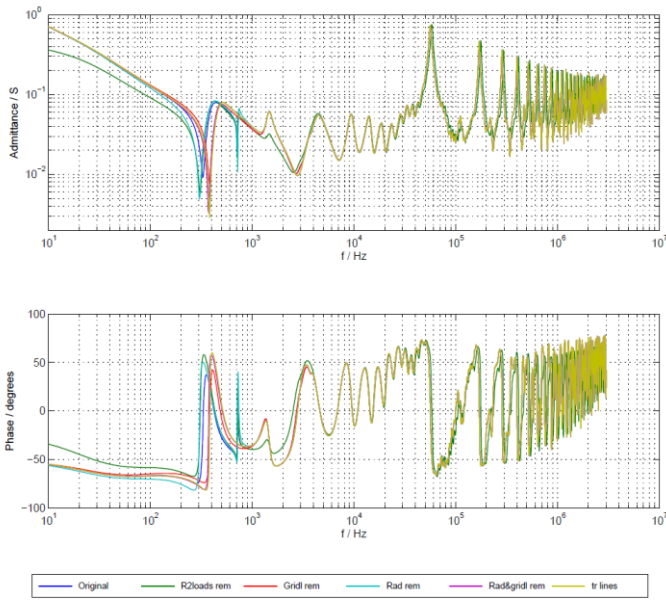
Fig. 6: Admittance scan at the middle radial at WT7 compared when configurations at the substation and wind turbines are made. *R2loads rem* - wind turbines auxiliary loads, filters and reactors are removed at the middle radial; *Gridl rem* - grid impedance disconnected; *Rad rem* - side radials are disconnected; *Rad&gridl rem* - side radials are disconnected, together with grid impedance removed; *tr lines* - transmission lines to external grid are removed, when side radials and grid impedance also are removed.

Fig. 7 shows how the admittance scan at the middle radial is affected by a change in radial topology. In this case, the last wind turbine (WT8) at the mentioned radial is disconnected. By removing the last wind turbine at the middle radial the admittance peaks above 10 kHz move to higher frequency range. The peaks distribution pattern seems to remain the same when the number of turbines connected at the radial gets from 8 to 7. The sharpest peaks in this case are at 49.4 kHz at WT6, 26.3 kHz at WT5 and 17.9 kHz at WT4.
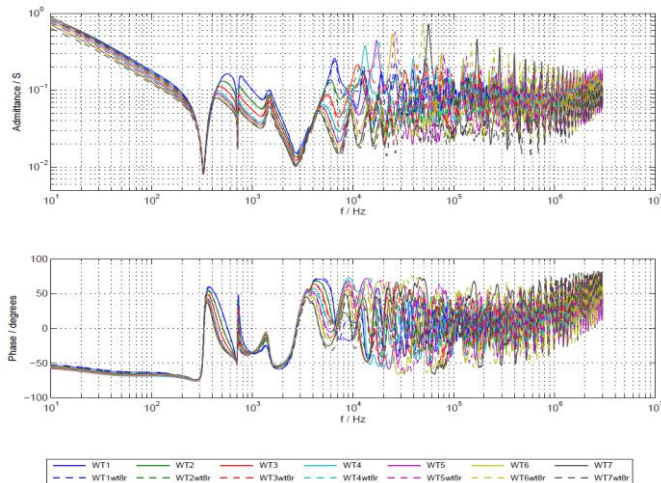

Fig. 7: Admittance scan at the middle radial at each wind turbine compared with admittance scan at each wind turbine at the middle radial when WT8 is removed. *WTn* – measurement location; *WTnwt8r* – modified measurement, where *n* is the wind turbine number.

Fig. 8 shows admittance scan at the low voltage side of wind turbine 1 at the middle radial. This shows high peaks at frequencies below 5 kHz which are determined by the high frequency filters. High frequency components are damped at this location.
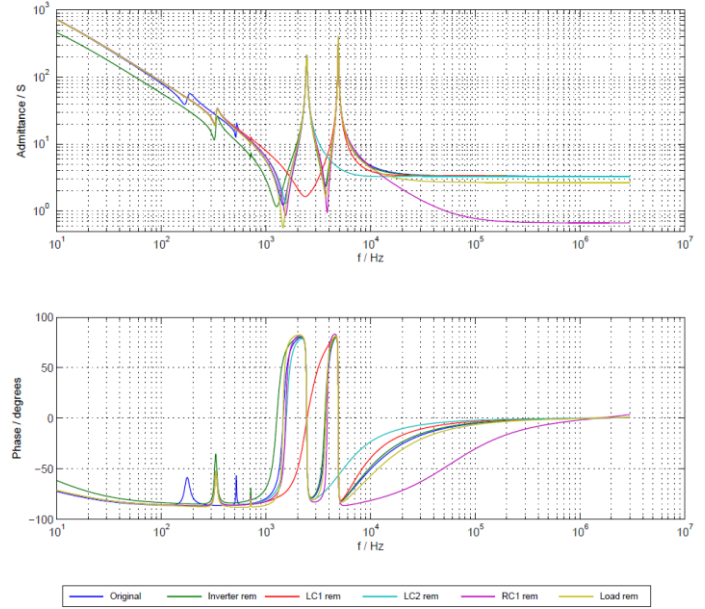

Fig. 8: Admittance scan at low voltage side of WT1's transformer with different configurations of LV components. *Inverter rem* - the inverter reactor is disconnected; *LC1 rem* - one of the high frequency filters is removed; *LC2 rem* - another high frequency filter is removed; *RC1 rem* - RC filter is removed; *Load rem* - auxiliary load at the low voltage side of wind turbine transformer is removed.

In order to give a general characterization of the frequency dependent admittances in the farm, an overview is given in Table 1 and Fig. 9, showing the admittance peaks determined at all wind turbines at the middle radial medium voltage side. It can be seen at which specific frequencies these peaks are appearing, if it is resonant or anti-resonant phenomena, and what the most dominant components are regarding their influence on a specific peak, including a description for each of the peak.

Table 1: Admittance peaks from all wind turbines at the middle radial description, characterization and component dependency.

| Peak	1p	2p	3p	4p	5p	6p	7p	8p
Frequency range (ELF-EHF)	ULF	ULF	ULF	VLF	VLF	VLF	VLF	LF
f / kHz	0.33	0.715	2.75	6.8	13.12	16.98	24.66	56.23
Resonance / anti-resonance	anti	anti	anti	res	res	res	res	res
Dominant components	WT transformer and cables	grid impedance	substation components	cable lengths	cable lengths	cable lengths	cable lengths	cable lengths
Dependent on	Most components	C bank and X/R ratio	Meas. location	Meas. location	Meas. location	Meas. location	Meas. location	Meas. location
Description	First peak	Second peak	Third peak	WT1 peak	WT4 peak	WT5 peak	WT6 peak	WT7 peak
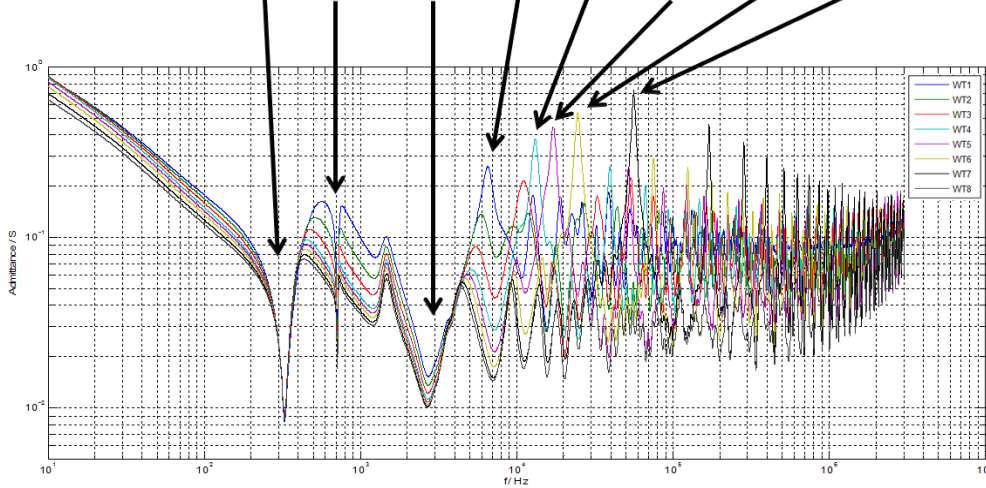
Fig. 9: Admittance scan at each wind turbine at middle radial.

B. Voltage transfer

Similar locations as in admittance sweeps were chosen for determination of the voltage transfer in order to be able to compare admittance and voltage, the latter being most relevant regarding overvoltages and insulation coordination.

Fig. 10 shows a voltage transfer peak at 229 Hz. Two dips are observed at frequencies below 5 kHz, indicating high frequency filters response. Peaks at higher frequencies are damped.
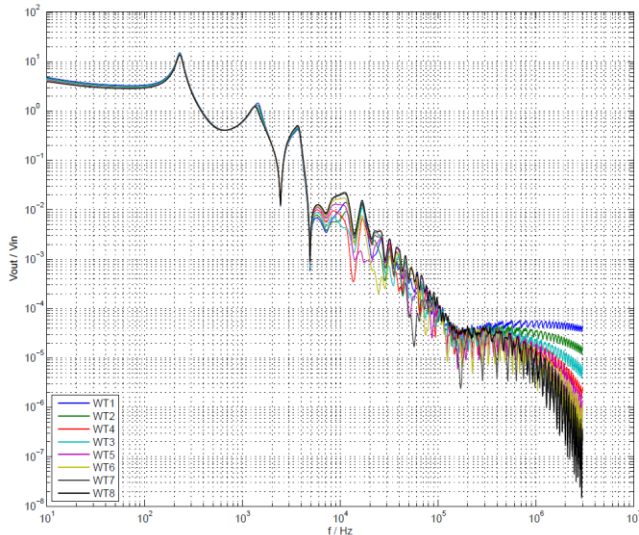

Fig. 10: Voltage transfer from LV side of WT1 to MV side of all the other turbines at the middle radial. *WTn* – measurement location, where n is the wind turbine number at the middle radial.

Fig. 11 shows voltage transfer dip at 1.45 kHz. It is followed by a transfer increase at the 2.72 kHz. Clear voltage transfer drops are observed at higher frequencies: sub-WT4 at 13.24 kHz, sub-WT5 at 17.21 kHz, sub-WT6 at 25 kHz, sub-WT7 at 56.75 kHz.
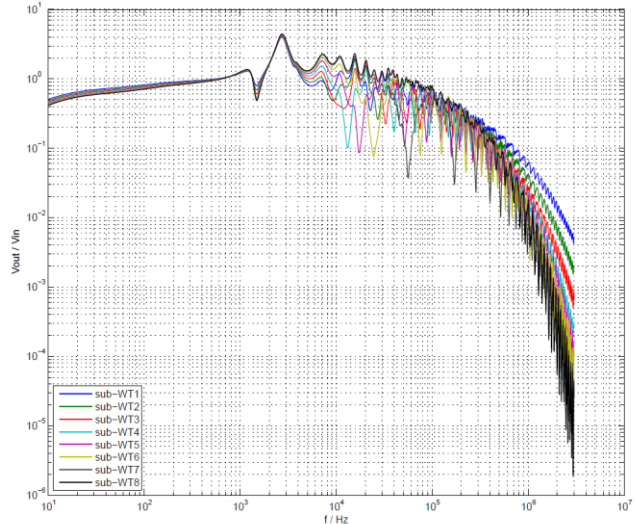

Fig. 11: Voltage transfer from substation medium voltage side to all turbines at the middle radial medium voltage side. *Sub* – substation; *WTn* – measurement location, where n is the wind turbine number at the middle radial.

In order to compare voltage transfer and admittance scans at different locations, similar peaks are investigated. In Fig. 10 the voltage transfer increase at 220 Hz can be directly compared with admittance decrease at 330 Hz seen in most of

the cases, where the following sharp voltage transfer dips are directly related to high frequency filters. In Fig. 11 the voltage transfer increases at 2.72 kHz showing a match with the admittance drop at 2.75 kHz observed at most of the locations. Similarly voltage drops at WT4 at 13.24 kHz, WT5 at 17.21 kHz, WT6 at 25 kHz, WT7 at 56.75 kHz are matching the admittance resonances at the same locations and frequencies. Clear deviation between the two methods investigated is visible, when directly comparing previously mentioned figures. Anti-resonances at frequencies below 2 kHz observed at admittance scans are not visible at the voltage transfer. On the other hand admittance resonant peaks and dips at higher frequencies do match the peaks and dips at voltage transfer.

VI. DISCUSSION

The study presented admittance scans and voltage transfers determined at different OWF locations. Electric components models were defined by the simulation software ATP-EMTP [5]. Components like capacitor bank represented as ideal capacitor or transformers were not represented by more detailed models due to lack of data.

Admittance scans at the collection grid medium voltage side showed resonances at higher frequencies which are influenced by the cables interconnecting wind turbines at the radials, whilst admittance at low voltage side of the wind turbines was purely dependent on high frequency filters with the high frequency components damped.

Direct comparison of admittance scans and voltage transfer showed some similar results indicating useful information by analyzing nodal admittances. Though, a direct one-to-one relation between all peaks in two methods cannot be applied, since not every peak from admittance scans matches the peaks at voltage transfer studies.

VII. CONCLUSIONS

A time domain offshore wind farm model was build and verified using ATP-EMTP software. Admittance scans and voltage transfer measurements were performed at different OWF locations.

Determination of the driving-point admittance at the substation showed capacitor bank dominance at this location. Admittance scans at the middle radial wind turbines medium voltage side showed three anti-resonant peaks, which were mainly dependent on onshore substation components, while sharp resonant peaks at higher frequencies were dominated by the cable section lengths interconnecting wind turbines. Admittance sweeps at the low voltage side of wind turbine 1 at the middle radial indicated two sharp resonant peaks determined by the high frequency filters, where high frequency components were damped.

Voltage transfer measurements showed an increase in voltage at a frequency comparable to the one obtained from admittance scan measurements. The influence of high frequency filters was clear when measuring voltage transfer from low voltage side of wind turbine 1 to medium voltage side of all other turbines at the middle radial. The transferred voltage from the medium voltage side of the substation to all turbines at the medium voltage side of middle radial indicated increases at 2.72 kHz at all locations and the voltage transfer drops at particularly WT4, WT5, WT6 and WT7 locations, which did match the admittance peaks from driving-point admittance measurements.

REFERENCES

[1] Poul Sørensen, Anca D. Hansen, Troels Sørensen, Christian S. Nielsen, Henny K. Nielsen, Leif Christensen, and Morten Ulletved, "Switching transients in wind farm grids", Risø National Laboratory, Technical University of Denmark, 2007.
[2] Bengt Franken, Henrik Breder, Mikael Dahlgren, and Erik K. Nielsen,"Collection grid topologies for off-shore wind parks", 18th International Conference and Exhibition on Electricity Distribution (CIRED 2005),(CP504),Volume 5, JUNE 2005.
[3] Andrzej Holdyk, Joachim Holboell, and Ivan Arana, "Compatibility between electric components in wind farms", 10th International Workshop on Large-Scale Integration of Wind Power into Power Systems as well as on Transmission Networks for Offshore Wind Farms in Aarhus, Denmark, October 2011.
[4] Andrzej Holdyk, Joachim Holboell, and Ivan Arana, "Validation of EMTP/ATP and PSCAD models of switching operation in the collection grid of Burbo Bank offshore wind farm", Technical University of Denmark, 2012.
[5] ATP-EMTP Rule Book.